Available online at www.sciencedirect.com
ScienceDirect
Vision Research 48 (2008) 626–634
Vision Research
www.elsevier.com/locate/visres

Morphology of age-related cuneiform cortical cataracts: The case for mechanical stress

Ralph Michael [a,*], Rafael I. Barraquer [a], Ben Willekens [b], Jan van Marle [c], Gijs F.J.M. Vrensen [d]

[a] Institut Universitari Barraquer, Research Department, Laforja 88, E-08021 Barcelona, Spain
[b] The Netherlands Institute for Neuroscience, Amsterdam, The Netherlands
[c] Department of Electron Microscopy, Academic Medical Center, University of Amsterdam, The Netherlands
[d] Department of Ophthalmology, Leiden University Medical Center, University of Leiden, The Netherlands

Received 25 May 2007; received in revised form 25 October 2007

Abstract

We evaluated the gross morphology, location, and fiber cell architecture of equatorial cortical opacities in the aging human lens. Using dark-field stereomicroscopy, we photographed donor lenses *in toto* and as thick slices. In addition, we investigated the details of the fiber cell architecture using fluorescent staining for membranes and by scanning electron microscopy. We then combined our data with data from recent studies on lens viscoelasticity. We found that small cortical and cuneiform opacities are accompanied by changes in fiber structure and architecture mainly in the equatorial border zone between the lens nucleus and cortex. Because the lens cortex and nucleus have different viscoelastic properties in young and old lenses, we hypothesize that external forces during accommodation cause shear stress predominantly in this border zone. The location of the described changes suggests that these mechanical forces may cause fiber disorganization, small cortical opacities, and ultimately, cuneiform cataracts.

Keywords: Cataract; Morphology; Presbyopia; Accommodation; Human

1. Introduction

Clinical observations have shown that the normal aging of the human lens, in the absence of disease, is accompanied by an increase in the overall light scattering of the lens. Until age 40, light scattering remains rather constant, thereafter increasing exponentially with age. This has been measured in donor lenses *in vitro* (van den Berg & Spekreijse, 1999) and *in vivo*, both for backward scattered light (Fujisawa & Sasaki, 1995; Hockwin, 1997; Sasaki, 1997; Sasaki, Sasaki, Jonasson, Kojima, & Cheng, 2004) and for forward scattered light (Franssen & Coppens, 2007; van den Berg, 1995; van den Berg et al., 2007). It has also been shown that, with age, coloration (or brunescence) of the lens nucleus occurs, which may increase from light yellow to dark brown (Lerman, 1980, 1989; Said & Weale, 1959); The possible underlying mechanisms of these processes include, in light scattering, the formation of protein aggregates and/or multilamellar bodies (Costello, Johnsen, Gilliland, Freel, & Fowler, 2007; van den Berg & Spekreijse, 1999) and, in brunescence, the formation of chromophores (Lerman, 1980, 1989; Truscott, 2000). Increased stray light and light absorption by chromophores reduce contrast sensitivity. In addition to these intracellular changes, the loss of transparency in the aging human lens and the different clinical types of cortical, nuclear, and subcapsular cataracts can be explained, at least in part, by changes in the architecture of the lens fibers (Phelps Brown & Bron, 1996).

Epidemiological studies using slit lamp and Scheimpflug camera observations have shown that, in developed

* Corresponding author. Fax: +34 93 414 1228.
E-mail address: ralphm@barraquer.com (R. Michael).

0042-6989/$ - see front matter © 2007 Elsevier Ltd. All rights reserved.
doi:10.1016/j.visres.2007.12.005

countries, cortical cataract is by far the most prevalent age-related cataract, 4–5 times more common than the onset of nuclear opacification (Hockwin, 1997; Sasaki, 1997; Sasaki et al., 2004). The most common types of cortical opacities share a basic morphology despite wide variations in shape and severity; they have been referred to in the literature as "wedge-shaped fiber opacities" (Fisher, 1973), "spoke-shaped opacities" (Brown, Vrensen, Shun-Shin, & Willekens, 1989), "cuneiform opacities" (Fisher, 1970), "water clefts" (Brown et al., 1993; Pau, 2006), and "supranuclear opacities" (Harding et al., 1985).

A possible relationship between cortical cataracts and mechanical stress has been suggested by Fisher (1970, 1973). According to Fisher, stress associated with accommodation forces inside presbyopic lenses might damage fibers and thus be responsible for spoke-shaped cataracts. Although others adhere to this theory (Pau, 2006; Pau & Kranz, 1991), Harding proposed an alternative mechanism by which cortical opacities are induced by the compaction of cortical fibers against the more resistant nucleus (Harding et al., 1985). In the present study, we focus on the morphology of a highly prevalent type of equatorial cortical opacity, observed in a large sample of donor lenses (Vrensen & Willekens, 1989), to uncover clues to the cause of its development.

2. Methods

Over a number of years, hundreds of human lenses were obtained from the Cornea Bank Amsterdam, headed by Dr. E. Pels, after the removal of corneas for transplantation purposes. Research using this material is in conformance with the Declaration of Helsinki and complies with Dutch regulations on the use of human postmortem and donor organs. In the present study, 39 lenses with representative opacities in their peripheries were selected for further evaluation (Figs. 1 and 2). The ages of the donors ranged between 55 and 90, and the postmortem time was between 5 and 24 h.

After dissection from the globe, all lenses were immediately photographed in frontal view with a Zeiss SV 8 stereomicroscope (Zeiss, Oberkochen, Germany) using dark-field illumination (Figs. 1 and 2). The lenses were then fixed for 7 days in a phosphate buffered solution containing 1.5% paraformaldehyde (pH 7.3) or in a cacodylate buffered solution containing 1.25% glutaraldehyde and 1.5% paraformaldehyde (pH 7.3). From 15 fixed lenses, axial slices of 1–2-mm thickness were cut using a sharp razor blade. These slices were examined using the same stereomicroscope and dark-field illumination. Morphological changes in theses slices were documented photographically (Fig. 3). The equatorial lens diameters and outer boundaries of the opacities were measured in the frontal view micrographs of the 39 intact lenses before fixation. In the 15 axial slices of fixed lenses, the distance between the lens border and the inner border of the opacity was measured. These measurements were taken manually from high quality printouts at about 10× magnification. Since it is known that lens tissue shrinks by 10–15% after fixation and dehydration (Michael, Vrensen, van Marle, Lofgren, & Soderberg, 2000), the distances measured in the fixed lenses are expressed as the percentage of the total lens diameter. In view of numerous studies using similar fixation protocols, it is extremely unlikely that the fiber alterations described in this paper are due to the shrinkage of lens tissue.

Areas on paraformaldehyde fixed lenses with specific opacities were dehydrated in a graded ethanol series and embedded in Technovit 7100 (Heraeus Kulzer GmbH, Wehrheim/TS, Germany). Sections of 1- to 2-μm thickness were cut and incubated with DiC18(3) fluorescent membrane dye (Fluka #42364, Sigma–Aldrich Co., St. Louis, MO, USA) in ethanol (80 μg/ml) for 30 min at room temperature and examined under a Leica TCS-NT laser scanning confocal microscope (Leica Laser Technik GmbH, Heidelberg, Germany; 550-nm excitation and 565-nm emission).

For scanning electron microscopy (SEM), regions with opacities in the glutaraldehyde/paraformaldehyde fixed lenses were cut into pieces, dehydrated in a graded ethanol series, and immersion dried in hexamethyldisilazane (Sigma, Dorset, UK). After evaporation of the drying agent on filter paper, the fragments were fractured, mounted with carbon glue on special stubs, and coated with ~7-nm platinum. The specimens were inspected and photographed using a Philips SEM 505 or Philips XL20 scanning electron microscope (Philips Industries, Eindhoven, The Netherlands).

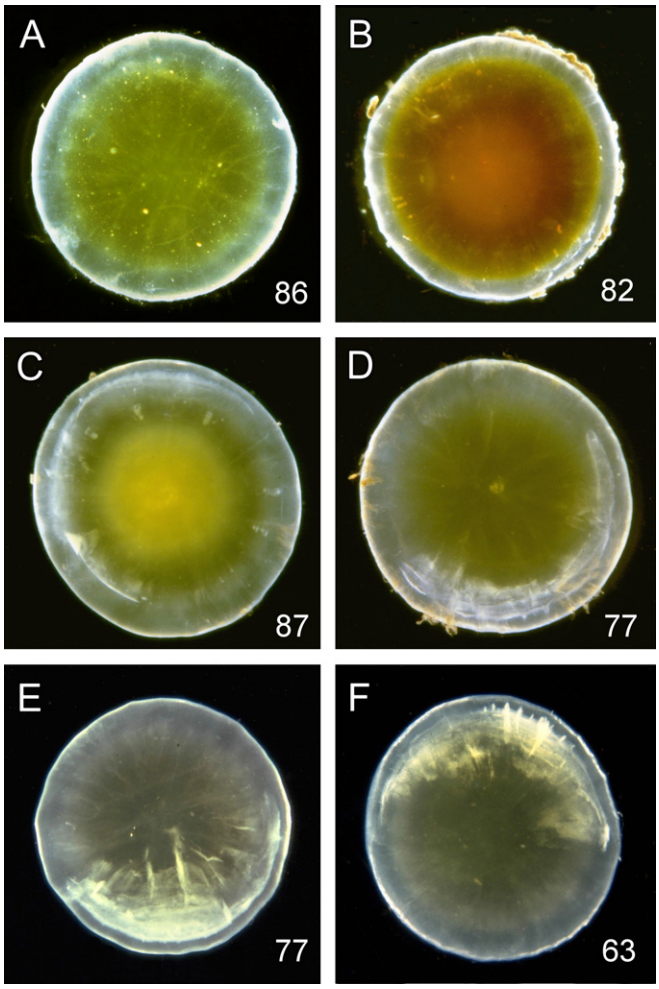

Fig. 1. Panel of dark-field micrographs of old human donor lenses, illustrating the presence of minor (A and B), mild (C and D), and more advanced (E and F) cortical opacities, restricted to a part of the lens. Photographs taken before lens fixation. The area between the outer limit of the opacity and the outer lens circumference is relatively transparent. Except for the spokes in (E), the opacities are outside the pupillary space and will not have seriously influenced the vision of these donors (without regard to nuclear opacity). *Note*: Numbers indicate the donor age.

3. Results

The dark-field micrographs in Figs. 1 and 2 show samples of the aging human donor lenses included in the present study. Most lenses exhibit nucleus coloration ranging

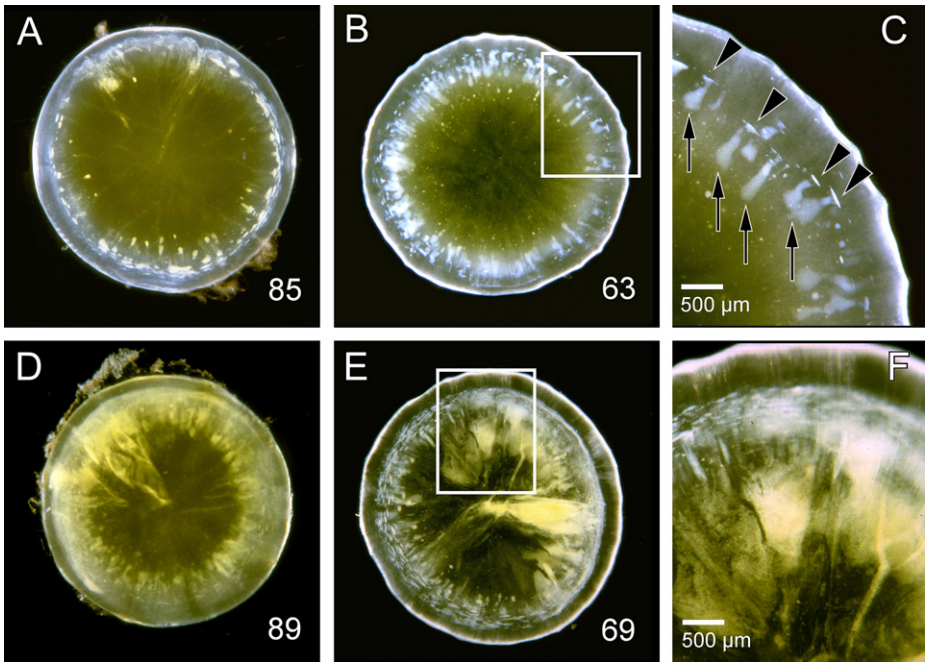

Fig. 2. Panel of dark-field micrographs of old human donor lenses, illustrating the presence of mild (A and B) and advanced (D and E) cortical opacities along the entire circumference of the lens. Photographs taken before lens fixation. In D and E, the opacities extend as spokes into the pupillary space and will likely have affected the vision of the donors. The space between the outer limit of the opacity and the lens circumference is relatively transparent, becoming especially evident at higher magnifications of the boxed areas in (B) and (E) (C and F, respectively). As seen in the overview micrographs of (A), (B), and (D), and especially evident at the higher magnification in (C), two types of opacities can be distinguished: (1) well-delineated, circular, line-like shades (arrows head) and (2) more diffuse radial shades (arrows). Radial and circular shades are often in close proximity. *Note*: Numbers indicate the donor age.

from pale yellow to dark brown. Furthermore, milky-white opacities appear in the equatorial cortical region. They vary from small isolated radial and circular shades (Figs. 1A–C and 2A–C) to broad, band-like opacities, sometimes extending as spokes into the axial region of the lens (Figs. 1D–F and 2D and E). When examined in more detail (Fig. 4), the small circular and radial shades of Figs. 1 and 2 appear to be located in the deep cortex, at or close to the area bordering the nucleus. The turbidity of these small shades is accompanied by a small number of aberrant fibers filled with globular material and surrounded by abnormal membranes. This means that small, as well as more extensive, opacities are restricted to the deeper cortical region and are bordered at the cortical and nuclear sides by unaffected, transparent groups of fibers.

The cortical opacities are restricted to one sector (Fig. 1) or cover the entire circumference of the lens (Fig. 2). It is also evident that the outermost cortical region is relatively transparent. This clear zone makes up approximately 10% of the lens radius, reaching a mean depth below the lens surface of 513 ± 26 µm ($n = 39$; ± 95% confidence interval) (Fig. 5). The equatorial lens diameter remained stable between ages 55 and 90, with a mean of 9.42 ± 0.15 mm ($n = 39$; ± 95% confidence interval); the outer diameter of the cortical opacities was also stable, measuring a mean 8.39 ± 0.12 mm ($n = 39$; ± 95% confidence interval) (Fig. 5). For technical reasons, we were unable to trace the orientation of the extracted lens relative to the globe of the eye and therefore cannot determine whether any quadrant is particularly affected. The results also show that nuclear coloration does not correlate with the severity of cortical opacities (Figs. 1 and 2).

Axial slices of lenses with distinct opacities extending towards the axial region (Fig. 3) confirm that, even in severe cases, the outermost equatorial cortical zone is relatively transparent. While the opacities extend in the anterior and/or posterior directions, in almost all cases, they spare the underlying nuclear region. Occasionally, a small wedge-shaped opacity can be seen penetrating the nuclear region at the equatorial plane (Fig. 3D). The border between the opaque, deep cortical fibers and the underlying clear nuclear material was sharp in all cases (Fig. 3). This inner border of the cortical opacities is located at $85.2\% \pm 1.5\%$ of the lens diameter ($n = 15$; ± 95% confidence interval). The data is expressed as percentage because it was measured in fixed lenses. Taking into account the mean lens diameter of fresh lenses, this corresponds to a mean depth of 697 ± 68 µm below the lens surface. This means the cortical opacity zone has an average thickness of about 200 µm in these cases.

Some areas within the cortical opacities showed undulated and folded fibers at the border zone between the cortex and nucleus in the pre-equatorial lens region overlying deeper (nuclear) layers that have normal fiber architecture (Fig. 6). We observed fiber undulations in 13 of 15 axial lens slices; we also observed fiber folds in 6 of 15 slices.

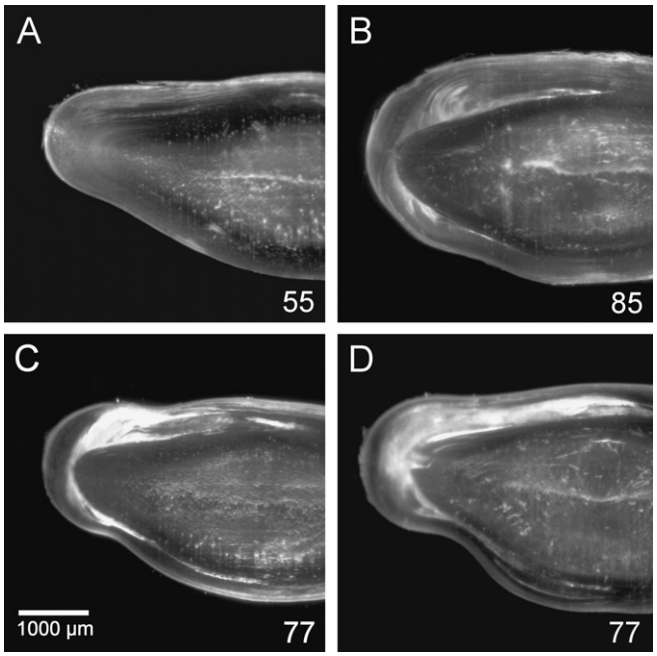

Fig. 3. Dark-field micrographs of slices cut in the axial plane of fixed donor lenses, without cortical opacities (A) and with advanced spokes (B–D), as illustrated in Figs. 1D–F and 2D and E. In addition to some irregular scattering due to imperfect slicing, the central nuclear parts of the slices are free of opacification. The peripheral opacities start abruptly at the border between the central (nuclear) and peripheral (cortical) regions of the lens. The opacities extend in the anterior (up) and posterior (down) directions. There is significant variability in the anterior/posterior extension of the opacities, as also shown in Figs. 1 and 2. The area occupied by the opacities is also variable and reflects the degree of opacification, as shown in Figs. 1 and 2. In a few cases, the opaque material seems to penetrate into the nuclear region (D). *Note*: Numbers indicate the donor age.

In addition, fluorescent microscopy revealed small spaces or clefts close to the folded and curled fibers (Fig. 6E). These spaces appear empty and are possibly filled with fluid *in vivo*. In all 15 cases, the opacities were bordered by regularly organized fibers on both the nuclear and cortical sides.

Altered lens fiber bundles seen in dark-field images were compared with SEM and fluorescent images (compare Fig. 7B with E and H, and Fig. 7C with F and J). Bundles of cortical fibers are often broken, with their ends perpendicular to the underlying nuclear fibers, which maintain a regular, uninterrupted organization (Fig. 7E and H). Such fiber breaks were seen in 13 of 15 axial lens slices. In 11 of these slices, broken cortical fibers appeared to form a wedge-shaped break in the lens cortex (Fig. 7C and F). In five cases, these breaks extended into the nuclear zone (Fig. 7J). When viewed with SEM at a particular angle (Fig. 8), the ends of the broken cortical fibers appeared sealed by membrane-like structures.

4. Discussion

The human donor lenses examined in the present *ex vivo* study, obtained from a large sample of lenses (Vrensen & Willekens, 1989), show small circular and radial opacities or shades in the equatorial and pre-equatorial regions at low magnification (dark-field photography, Figs. 1, 2, and 4A and B), at or close to the border between the cortex and adult nucleus (Taylor et al., 1996). These kinds of changes were previously described in detail by Obazawa, Fujiwara, and Kawara (1983) and later by Vrensen and Willekens (1990). They are very common, appearing exclusively as cortical opacities at a prevalence of approximately 30% of the population over age 45 (Vrensen & Willekens, 1989). The fibers in these areas are filled with globular material and bordered by abnormal membranes (Fig. 4) (Vrensen & Duindam, 1995; Vrensen, Van Marle, Willekens, & Van Veen, 1990; Vrensen & Willekens, 1990). Our observations, as well as those in previous studies (Vrensen & Willekens, 1989; Willekens, Kappelhof, & Vrensen, 1987), confirm that most of these opacities lay outside the pupillary area, even during spontaneously occurring mydriasis, and are unlikely to affect vision. Otherwise, radial and circular shades are found in conjunction with more extensive peripheral band-like and/or spoke-like opacities, the latter often extending into the pupillary space. The prevalence of these more extensive opacities dramatically increases from about 10% of people under age 45 to 40–45% in those over age 60 (Vrensen & Willekens, 1989). While these cortical opacities can be either restricted to a sector or quadrant or found around the entire circumference of the lens, their extent is not directly related to lens age.

Although all 39 lenses studied have opacities located in the pre-equatorial and equatorial regions at the border between nucleus and cortex, each lens is different in terms of the area affected and severity. The differences between lenses could be interpreted as different stages of the same phenomenon. The development of cortical opacities seems to start in the anterior and posterior pre-equatorial zones. The first signs might be small numbers of opaque fiber bundles (Fig. 3B), which develop into larger opaque areas and extend towards the lens pole and lens equator (Fig. 3C), finally progressing to thicker and denser opacities (Fig. 3 D) covering the entire equatorial and pre-equatorial zones and sometimes extending into the pupillary area. However, there is always a clear zone between the opacities and the lens surface at the equator, and, while the equatorial diameter did not change in the age bracket studied (55 to 90) (Willekens et al., 1987), the outer limit of the opacities remained at a constant depth of about 500 µm below the lens surface (Fig. 5). There is also a sharp inner limit of the opacities at the equator, at a mean depth of about 700 µm, corresponding to the border between the cortex and adult nucleus.

SEM revealed small and large groups of cortical fibers with broken ends in the pre-equatorial zone at a depth corresponding to the cortical/nuclear interface (Fig. 7E and F, and Fig. 6B and C). The portions of these fibers posterior and/or anterior to the breaks appeared folded and undulated, while both the deeper nuclear and more superficial

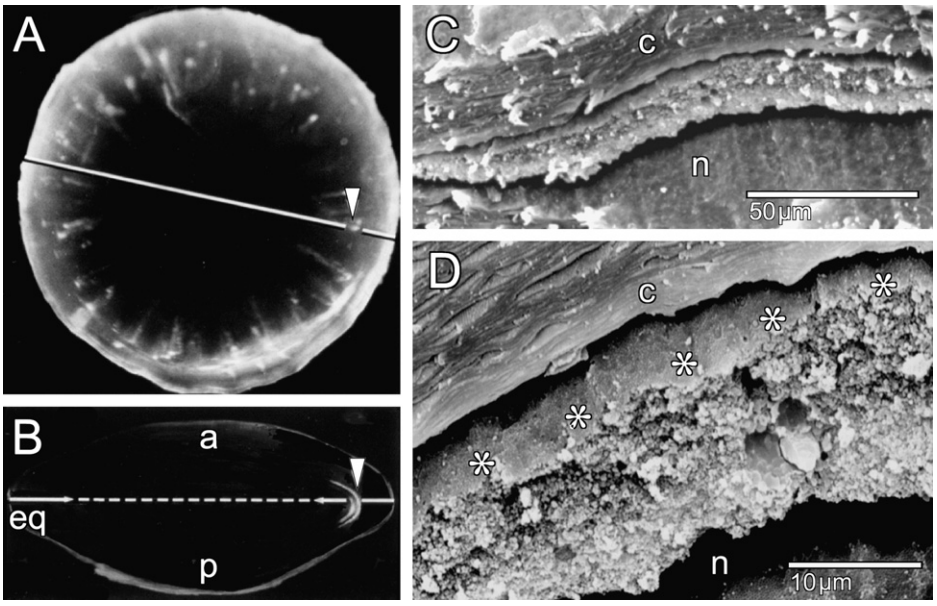

Fig. 4. Dark-field micrograph of the frontal view (A) of a donor lens with minor peripheral opacities. The central slice along the line indicated in (A) shows two well-delineated opacities (arrow heads) at a border zone between the central (nuclear) and equatorial cortical parts (B). The low-power SEM image (C) of the fractured pieces of lenses with minor opacities, as shown in (A) and (B). The opacities consist of disturbed lens material bordered by unaffected fibers, both on the nuclear and cortical sides. At high power (D), it can be seen that the disturbed lens material is formed by lens fibers with aberrant membranes (asterisks) and are filled with globular material. *Note*: Eq, equator; n, nuclear side; C, cortical side.

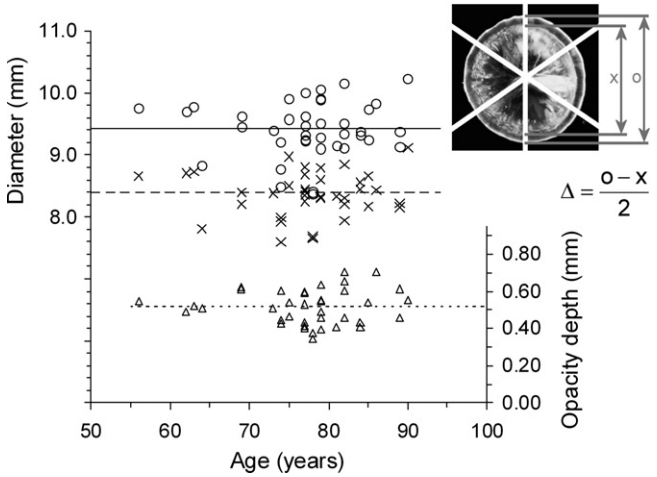

Fig. 5. Equatorial lens diameter (○) and outer diameter of cortical opacities (×) (left *y*-axis), as measured in frontal view dark-field micrographs (insert) before lens fixation. Each data point represents the mean of three measurements (white lines of the insert). The opacity depth below the lens surface (Δ) is given as half the difference between the lens diameter and the outer diameter of the cortical opacities (right *y*-axis).

neighboring cortical fibers exhibited normal structure and architecture. The sealed ends of the broken fibers (Fig. 8) might explain why these fibers remain arranged regularly and mutually connected despite their breaks; the sealed ends might also explain the lack of involvement of neighboring fibers. This is consistent with, and may in part explain, the generally slow progression of cortical opacities (Phelps Brown & Bron, 1996). Fluorescence microscopy (DiI) (Fig. 7H and J, Fig. 6D and E) supports the SEM findings of broken, folding, and undulating fibers in this border region, additionally showing the presence, between the aberrant fibers, of small and large spaces that appear filled with fluid. This would be in line with the clinical description of "water clefts" associated with cortical opacities (Brown et al., 1993; Pau, 2006).

A major conclusion of the present morphological study is that cortical opacities mostly occur at the equatorial and pre-equatorial border of the lens cortex and adult nucleus, while the deeper and more superficial layers neighboring these opacities remain relatively unaffected. The appearance of disorganized fiber cell architecture within cortical opacities suggests that mechanical forces (for instance shearing) may play a role in the formation of this type of cortical cataract. In particular, the broken undulated and S-shaped fibers (Fig. 6) hint at the action of "longitudinal" forces. As proposed by Fisher and other investigators (Fisher, 1970, 1973; Pau, 2006; Pau & Kranz, 1991), accommodation could be the origin of these forces. Furthermore, the precise location of the changes at the cortical/nuclear interface may be related to mechanical (viscoelastic) or structural differences between these layers and be the possible source of the accommodation-related stresses.

The lens cortex and nucleus are known to have different viscoelastic properties. The stiffness of the lens nucleus and cortex is generally believed to increase with age. Using a spinning technique, Fisher (1971) found that Young's modulus is generally higher in the lens cortex than in the nucleus, the latter steadily increasing after age 40 and approaching the cortical stiffness values by age 70. According to more recent evidence, based on measurements with dynamic mechanical analyzers (Heys, Cram, & Truscott,

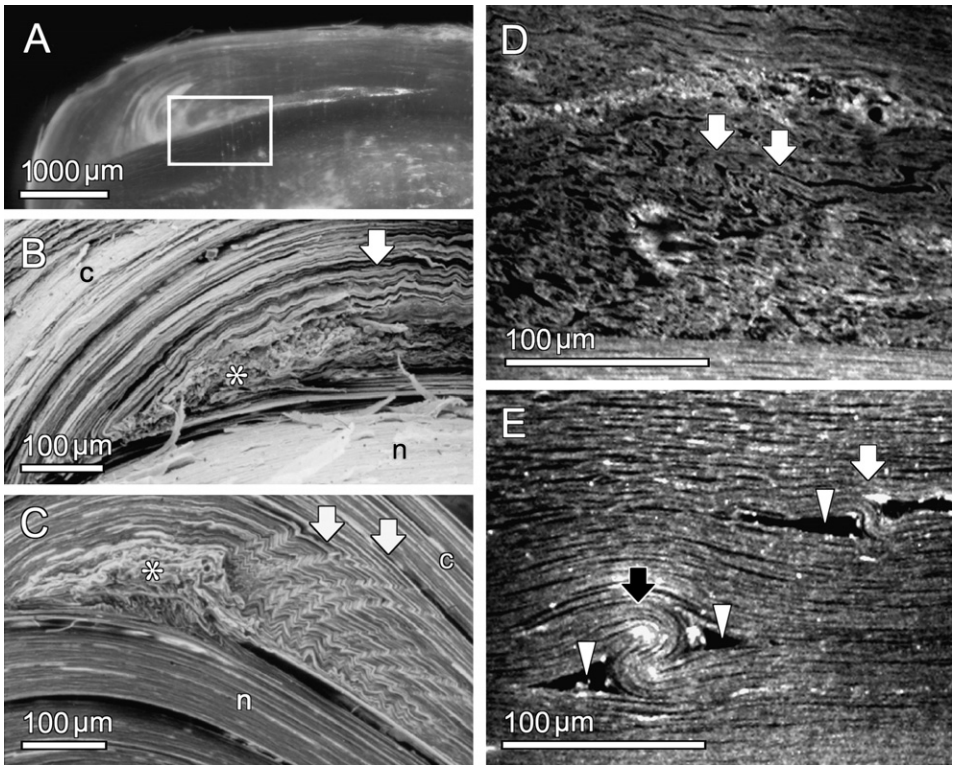

Fig. 6. Examples of folded (white arrows), S-shaped (black arrow), and curled (asterisks) fibers, as they appear in SEM (B and C) and fluorescence (D and E) images of a pre-equatorial cortical opacity, illustrated in (A). Note that the nuclear and superficial cortical fibers are neatly organized (B and C). In (E), small dark regions (arrowheads) most likely reflect the presence of water spaces that form next to folded and S-shaped fiber bundles. *Note*: n, nuclear side; C, cortical side.

2004; Weeber, Eckert, Pechhold, & van der Heijde, 2007), and in contrast with previous observations by Fisher (1971), the difference in stiffness between the human lens nucleus and cortex, as indicated by their respective shear moduli, decreases until equalizing in about the fourth decade of life. However, because of a progressive rise in the nuclear shear modulus, the difference increases again from the fifth decade onwards. When measured across an equatorial section (Heys et al., 2004), the variation in shear modulus is relatively small in young lenses (age 19), with significantly higher values in the cortical region. However, in older lenses (age 64), the ratio is reversed, with shear moduli much higher in the nucleus than in the cortex (Heys et al., 2004). Scheimpflug photography and magnetic resonance imaging indicate that the increase in axial lens thickness during accommodation is mainly due to thickening of the lens nucleus (Brown, 1973; Dubbelman, van der Heijde, Weeber, & Vrensen, 2003; Koretz, Cook, & Kaufman, 2002; Strenk et al., 1999). Indeed, densitometric data from Scheimpflug images show that about 90% of the increase in lens thickness during accommodation takes place in the nucleus (Dubbelman et al., 2003). The lower level of stiffness of the nucleus compared to that of the cortex in pre-presbyopic lenses is consistent with these findings. The high nuclear stiffness of presbyopic lenses is consistent with the general understanding that accommodation is virtually zero in old age. Interestingly, Dubbelman et al. (2003) found a "sudden change in stretch at the transition between anterior cortex and nucleus".

It has been suggested that the increase in stiffness and, therefore, the increase in shear modulus between the cortex and nucleus are caused by the compaction of the nuclear fibers, in itself due to an age-related increase in protein content. Indeed a significant increase in nuclear protein content has been measured in rat, bovine, and rabbit lenses (Huizinga, Bot, de Mul, Vrensen, & Greve, 1989; Philipson, 1969; Pierscionek & Augusteyn, 1992), and it has been inferred from refractive index measurements in rats (Campbell, 1984; Pierscionek, Smith, & Augusteyn, 1987). Moreover, several studies of human lenses (Fagerholm, Philipson, & Lindström, 1981; Huizinga et al., 1989; Siebinga, Vrensen, De Mul, & Greve, 1991) show that protein content rises in the outer layers of young lenses, from about 18% to 35–40% within 0.2 mm from the anterior surface and within 0.7 mm from the equatorial surface, the latter concentration remaining relatively constant throughout the rest of the lens. With age, the increase in protein content in the superficial equatorial region becomes significantly steeper (Siebinga et al., 1991). This has recently been confirmed in an *in vitro* MRI study of human lenses showing that the refractive index profile, which correlates with protein content, in the equatorial region is significantly steeper in old lenses (age 82), compared to young lenses (age 7) (Jones, Atchison, Meder, &

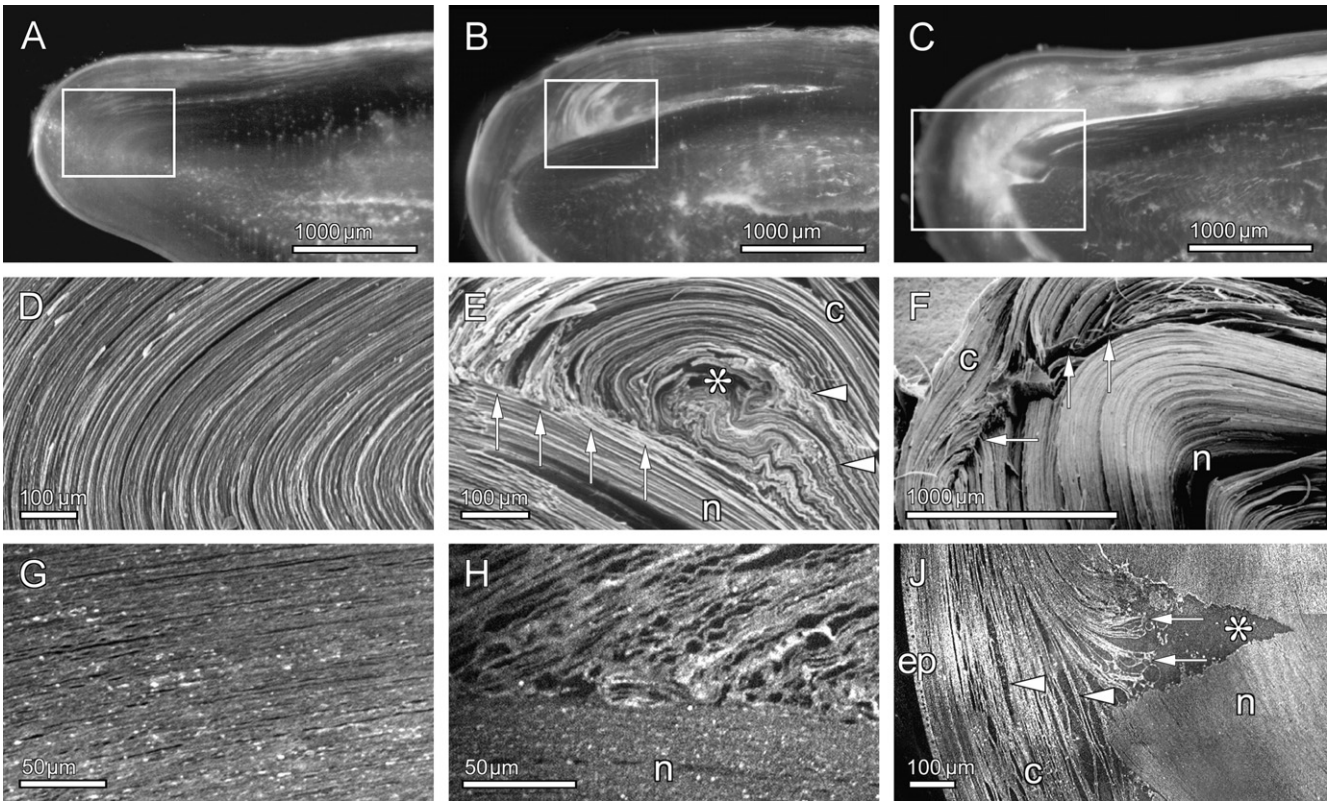

Fig. 7. Fiber organization in a lens without cataract (A) and in two cases of cortical opacities (boxed areas in B and C), as visualized by SEM (D–F) and fluorescence histology (G, H, and J). It is shown in (E) that fibers at the border zone between the nuclear and cortical lens regions is broken (arrows) and that the broken ends are directed against the nuclear fibers, which maintain a regular, uninterrupted organization. Further, note the curled (asterisk) and folded (arrowheads) fibers in the region adjoining the broken fibers. Fluorescence histology of this type of opacification (H) shows the oblique orientation of the broken fibers on the regularly organized nuclear fibers. The dark regions in the fluorescence micrograph indicate the presence of spaces likely filled with fluid. The SEM micrograph of (F) shows broken fibers at several places (arrows) in the border zone between the cortex and nucleus. The nuclear fibers are regularly organized, as are the more superficial cortical fibers bridging the break zone. The fluorescence micrograph (J) shows the nuclear fibers and the most superficial fibers, which are regularly organized. The fibers between these layers are partly separated by water lakes (arrowheads). Some are broken (arrows), and there is a large triangular region (asterisk) (cf. F) free of fibers, most likely filled with fluid. *Note*: Ep, epithelium, n, nuclear side; C, cortical side.

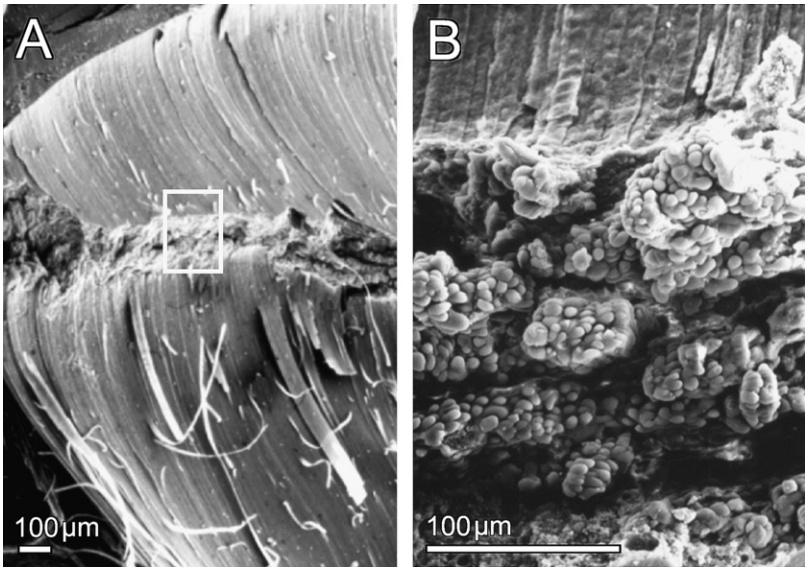

Fig. 8. Low-power (A), frontal SEM view of broken fibers in a deeper area of the equatorial plane of a human lens, with an opacity comparable to that illustrated in Fig. 3B. Note the circumferential width over which the fibers are broken. The appearance of the broken ends of the fibers in the higher power view (B) seems to indicate that they are sealed by membrane-like structures.

Pope, 2005). This means that lens fiber compaction due to an increase in protein concentration may partly be responsible for the dramatic rise in nuclear shear moduli in aging presbyopic human lenses, especially in the equatorial region. Additional explanations of the different elastic properties suggest changes in the macromolecular organization of intracellular proteins and changes in the architectural organization of the lens fibers (Al-Ghoul et al., 2001).

In a sample of many hundreds of lenses taken from human donor eyes, it was revealed that small radial and circular shades and more extensive band- and spoke-like equatorial opacities are highly prevalent, increasing from ~30% in 31–45-year-olds to ~75% in 76–90-year-olds; (Vrensen & Willekens, 1989). Our histological and SEM studies of 39 representative lenses, taken from this population, reveal that the strong light scattering properties of these opacities and cataracts are due to more or less severe changes in the structure and architecture of the lens fibers. These changes are mostly located on the border between the equatorial cortex and nucleus. The overlying cortical and underlying nuclear fibers exhibit normal structure and architecture. The fiber pathology observed, especially broken and undulating fibers, suggests that age-related differences in the viscoelastic properties at the cortical/nuclear interface might be responsible for stress on the lens fibers during accommodation, leading to these irreversible changes and cataracts. As outlined above, there is ample evidence that aging of the human lens is accompanied by changes in viscoelastic properties and that, over age 40–50, the nucleus becomes significantly stiffer than the cortex. This is most likely due to a steeper increase in protein content and macromolecular and structural changes, especially at the equator. This means that accommodation forces exerted by zonular fibers function differently in young and presbyopic lenses. This is supported by the fact that, in old presbyopic lenses, the change in axial thickness, and thus in accommodation, which is mainly due to increased nuclear thickness, becomes virtually zero.

Based on the evidence presented in this paper, it would be reasonable to hypothesize that differential, age-related changes in the viscoelastic properties of the nucleus and cortex of the lens are responsible for mechanical stress on the fibers at the interface between both compartments and that this leads to the equatorial opacities and cataracts described. However, the exact mechanism of their formation cannot be revealed from morphological observations alone. Further biomechanical analysis is needed, including analysis of the actual complexities, heterogeneities, and anisotropies inside the crystalline lens.

References

Al-Ghoul, K. J., Nordgren, R. K., Kuszak, A. J., Freel, C. D., Costello, M. J., & Kuszak, J. R. (2001). Structural evidence of human nuclear fiber compaction as a function of ageing and cataractogenesis. *Experimental Eye Research, 72*, 199–214.

Brown, N. (1973). The change in shape and internal form of the lens of the eye on accommodation. *Experimental Eye Research, 15*, 441–459.

Brown, N. P., Harris, M. L., Shun-Shin, G. A., Vrensen, G. F., Willekens, B., & Bron, A. J. (1993). Is cortical spoke cataract due to lens fibre breaks? The relationship between fibre folds, fibre breaks, waterclefts and spoke cataract. *Eye, 7*, 672–679.

Brown, N. P., Vrensen, G., Shun-Shin, G. A., & Willekens, B. (1989). Lamellar separation in the human lens: The case for fibre folds. A combined in vivo and electron microscopy study. *Eye, 3*, 597–605.

Campbell, M. C. (1984). Measurement of refractive index in an intact crystalline lens. *Vision Research, 24*, 409–415.

Costello, M. J., Johnsen, S., Gilliland, K. O., Freel, C. D., & Fowler, W. C. (2007). Predicted light scattering from particles observed in human age-related nuclear cataracts using mie scattering theory. *Investigative Ophthalmology and Visual Science, 48*, 303–312.

Dubbelman, M., van der Heijde, G. L., Weeber, H. A., & Vrensen, G. F. (2003). Changes in the internal structure of the human crystalline lens with age and accommodation. *Vision Research, 43*, 2363–2375.

Fagerholm, P. P., Philipson, B. T., & Lindström, B. (1981). Normal human lens - the distribution of protein. *Experimental Eye Research, 33*, 615–620.

Fisher, R. F. (1970). Senile cataract. A comparative study between lens fibre stress and cuneiform opacity formation. *Transactions of the Ophthalmological Societies of the United Kingdom, 90*, 93–109.

Fisher, R. F. (1971). The elastic constants of the human lens. *Journal of Physiology (London), 212*, 147–180.

Fisher, R. F. (1973). Human lens fibre transparency and mechanical stress. *Experimental Eye Research, 16*, 41–49.

Franssen, L., Coppens, J. (2007). Straylight at the retina—scattered papers. PhD Thesis. Amsterdam, Universiteit van Amsterdam, pp. 1–302.

Fujisawa, K., & Sasaki, K. (1995). Changes in light scattering intensity of the transparent lenses of subjects selected from population-based surveys depending on age: Analysis through Scheimpflug images. *Ophthalmic Research, 27*, 89–101.

Harding, C. V., Susan, S. R., Lo, W.-K., Bobrowski, W. F., Maisel, H., & Chylack, L. T. (1985). The structure of the human cataractous lens. In H. Maisel (Ed.), *The ocular lens: Structure, function, and pathology* (pp. 367–404). New York: Marcel Dekker.

Heys, K. R., Cram, S. L., & Truscott, R. J. (2004). Massive increase in the stiffness of the human lens nucleus with age: The basis for presbyopia? *Molecular Vision, 10*, 956–963.

Hockwin, O. (1997). Multifactorial pathogenesis of "Senile Cataract". In G. Glaesser, O. Hockwin, & G. F. J. M. Vrensen (Eds.). *Eye lens epithelium: Damaging mechanisms and lens transparency* (Vol. 299, pp. 37–44). Halle: Nova Acta Leopoldina NF 75.

Huizinga, A., Bot, A. C., de Mul, F. F., Vrensen, G. F., & Greve, J. (1989). Local variation in absolute water content of human and rabbit eye lenses measured by Raman microspectroscopy. *Experimental Eye Research, 48*, 487–496.

Jones, C. E., Atchison, D. A., Meder, R., & Pope, J. M. (2005). Refractive index distribution and optical properties of the isolated human lens measured using magnetic resonance imaging (MRI). *Vision Research, 45*, 2352–2366.

Koretz, J. F., Cook, C. A., & Kaufman, P. L. (2002). Aging of the human lens: Changes in lens shape upon accommodation and with accommodative loss. *Journal of the Optical Society of America [A], 19*, 144–151.

Lerman, S. (1980). *Radiant energy and the eye*. New York: Macmillan, pp. 115–186.

Lerman, S. (1989). In vivo lens fluorescence as a cataract marker. *Developments in Ophthalmology, 17*, 60–64.

Michael, R., Vrensen, G. F., van Marle, J., Lofgren, S., & Soderberg, P. G. (2000). Repair in the rat lens after threshold ultraviolet radiation injury. *Investigative Ophthalmology and Visual Science, 41*, 204–212.

Obazawa, H., Fujiwara, T., & Kawara, T. (1983). The maturing process of the senile cataractous lens. In P. Henkind (Ed.), *Acta XXIV international congress of ophthalmology. American academy of ophthalmology*. Philadelphia: JB Lippincott.

Pau, H. (2006). Cortical and subcapsular cataracts: Significance of physical forces. *Ophthalmologica, 220*, 1–5.

Pau, H., & Kranz, J. (1991). The increasing sclerosis of the human lens with age and its relevance to accommodation and presbyopia. *Graefes Archive for Clinical and Experimental Ophthalmology, 229*, 294–296.

Phelps Brown, N. P., & Bron, A. J. (1996). *Lens Disorders A Clinical Manual of Cataract Diagnosis*. Oxford: Butterworth-Heinemann.

Philipson, B. (1969). Distribution of protein within the normal rat lens. *Investigative Ophthalmology, 8*, 258–270.

Pierscionek, B. K., & Augusteyn, R. C. (1992). Growth related changes to functional parameters in the bovine lens. *Biochimica et Biophysica Acta, 1116*, 283–290.

Pierscionek, B., Smith, G., & Augusteyn, R. C. (1987). The refractive increments of bovine alpha-, beta-, and gamma-crystallins. *Vision Research, 27*, 1539–1541.

Said, F. S., & Weale, R. A. (1959). The variation with age of the spectral transmissivity of the living human crystalline lens. *Gerontologia, 3*, 213–231.

Sasaki, K. (1997). Epidemiology - Search for risk factors of cataract formation. In G. Glaesser, O. Hockwin, & G. F. J. M. Vrensen (Eds.). *Eye lens epithelium: Damaging mechanisms and lens transparency* (Vol. 299, pp. 25–36). Halle: Nova Acta Leopoldina NF 75.

Sasaki, K., Sasaki, H., Jonasson, F., Kojima, M., & Cheng, H. M. (2004). Racial differences of lens transparency properties with aging and prevalence of age-related cataract applying a WHO classification system. *Ophthalmic Research, 36*, 332–340.

Siebinga, I., Vrensen, G. F., De Mul, F. F., & Greve, J. (1991). Age-related changes in local water and protein content of human eye lenses measured by Raman microspectroscopy. *Experimental Eye Research, 53*, 233–239.

Strenk, S. A., Semmlow, J. L., Strenk, L. M., Munoz, P., Gronlund-Jacob, J., & DeMarco, J. K. (1999). Age-related changes in human ciliary muscle and lens: A magnetic resonance imaging study. *Investigative Ophthalmology and Visual Science, 40*, 1162–1169.

Taylor, V. L., Al-Ghoul, K. J., Lane, C. W., Davis, V. A., Kuszak, J. R., & Costello, M. J. (1996). Morphology of the normal human lens. *Investigative Ophthalmology and Visual Science, 37*, 1396–1410.

Truscott, R. J. (2000). Age-related nuclear cataract: A lens transport problem. *Ophthalmic Research, 32*, 185–194.

van den Berg, T. J. T. P. (1995). Analysis of intraocular straylight, especially in relation to age. *Optometry and Vision Science, 72*, 52–59.

van den Berg, T. J., & Spekreijse, H. (1999). Light scattering model for donor lenses as a function of depth. *Vision Research, 39*, 1437–1445.

van den Berg, T. J., Van Rijn, L. J., Michael, R., Heine, C., Coeckelbergh, T., Nischler, C., et al. (2007). Straylight Effects with Aging and Lens Extraction. *American Journal of Ophthalmology, 144*, 358–363.

Vrensen, G. F., & Duindam, H. J. (1995). Maturation of fiber membranes in the human eye lens. Ultrastructural and Raman microspectroscopic observations. *Ophthalmic Research, 27*(Suppl 1), 78–85.

Vrensen, G., Van Marle, J., Willekens, B., & Van Veen, H. (1990). Square arrays in early cortical lens opacities. *Investigative Ophthalmology and Visual Science, 31*, 2476–2481.

Vrensen, G., & Willekens, B. (1989). Classification and prevalence of early senile lens opacities in human donor eyes. *Developments in Ophthalmology, 17*, 181–187.

Vrensen, G., & Willekens, B. (1990). Biomicroscopy and scanning electron microscopy of early opacities in the aging human lens. *Investigative Ophthalmology and Visual Science, 31*, 1582–1591.

Weeber, H. A., Eckert, G., Pechhold, W., & van der Heijde, R. G. (2007). Stiffness gradient in the crystalline lens. *Graefes Archive for Clinical and Experimental Ophthalmology, 245*, 1357–1366.

Willekens, B., Kappelhof, J., & Vrensen, G. (1987). Morphology of the aging lens. I. Biomicroscopy and biometrics. *Lens Research, 4*, 207–230.